Journal of Solid State Chemistry 182 (2009) 2626–2631

Contents lists available at ScienceDirect

Journal of Solid State Chemistry

journal homepage: www.elsevier.com/locate/jssc

Structural phase transitions in the relaxor ferroelectric $Pb_2Bi_4Ti_5O_{18}$

Richard J. Goff, Philip Lightfoot *

EaStChem, School of Chemistry, University of St. Andrews, St. Andrews, Fife, KY16 9ST, UK

ARTICLE INFO

Article history:
Received 17 March 2009
Received in revised form
22 June 2009
Accepted 25 June 2009
Available online 30 June 2009

Keywords:
Ferroelectric
Relaxor
Aurivillius phase
Powder neutron diffraction
Phase transitions

ABSTRACT

The relaxor ferroelectric $Pb_2Bi_4Ti_5O_{18}$ has been studied by Rietveld refinement of powder neutron diffraction data collected at temperatures of 100, 250 and 400 °C. Our refinements are compatible with the 'average' crystal structure of $Pb_2Bi_4Ti_5O_{18}$ undergoing the phase transition sequence $F2mm \rightarrow I4mm \rightarrow I4/mmm$ as a function of increasing temperature, with the latter phase being observed above the known ferroelectric Curie temperature, T_m, and the intermediate phase consistent with a previously observed dielectric anomaly around 207 °C. The results are, however, in conflict with both observation of a symmetry lowering (to space group B2eb) in the lowest temperature phase, observed by electron diffraction, and also with electrical property measurements, which suggest both *a*- and *c*-axis polarisation up to T_m. Nevertheless, these crystallographic results are consistent with the observation of relaxor behaviour in this material, and underline the importance of considering 'long-range' versus 'local' structural effects in relaxor materials.

1. Introduction

The Aurivillius family of layered bismuth-containing oxides encompasses many ferroelectric materials, which have recently attracted considerable attention due to their remarkable fatigue resistance [1,2]. Aside from their potential and realised technological significance, this family of materials exhibit fascinating and complex structural chemistry. Structurally, they may be considered as layered intergrowths of fluorite like $[M_2O_2]$ units alternating with perovskite-like $[A_{n-1}B_nO_{3n+1}]$ units to give a general composition $M_2A_{n-1}B_nO_{3n+3}$, where M is generally Bi^{3+}, A is a group II or lanthanide metal and B is a d^0 transition element (Ti^{4+}, Nb^{5+}, Ta^{5+}, etc.). For differing numbers of perovskite layers, *n*, typical Aurivillius phases are Bi_2WO_6 ($n=1$), $SrBi_2Ta_2O_9$ ($n=2$), $Bi_4Ti_3O_{12}$ ($n=3$), $BaBi_4Ti_4O_{15}$ ($n=4$) and $Ba_2Bi_4Ti_5O_{18}$ ($n=5$).

In recent years the detailed crystallographic behaviour of these materials has been steadily unravelled, principally by powder neutron diffraction (PND) [3–5], and also by complementary electron diffraction [6], single crystal X-ray [7,8] and synchrotron X-ray powder diffraction methods [9]. All members of the series may be considered as deriving from an archetypal parent structure which would be paraelectric and, ideally, adopt the tetragonal space group *I*4/*mmm*. In the phases generally observed at ambient temperatures there are significant deviations from this ideal parent structure, and it is these deviations which give rise to the ferroelectric behaviour. The principal distortion mode which prompts ferroelectricity is a polar displacement of ions along a direction perpendicular to the layer direction (*c*-axis), which is generally defined as the *a*-axis. However, the other distortion mode which is generally possible is an 'octahedral tilt' mode. Both these distortions reduce the symmetry of the parent *I*4/*mmm* phase to orthorhombic. In the general case there is no fundamental reason why these two distortion modes should become active at the same temperature [10]; indeed there are now several well-characterised examples of 'two-step' phase transitions, whereby the tilt mode freezes out first, on cooling from the paraelectric phase, followed at a lower temperature by activation of the ferroelectric displacement mode [3,11,12]. There are also examples where this phenomenon has been searched for, but appears to be absent [13,14]. Detailed group-theoretical analyses on the $n=2$ phase $SrBi_2Ta_2O_9$ [15] and the $n=3$ phase $Bi_4Ti_3O_{12}$ [10] suggest contrasting behaviour in the sequence of mode instabilities, i.e. for $n=2$ the tilt mode is the least stable, whereas for $n=3$ the displacement mode is the least stable. This leads to prediction of opposing sequences of phase transitions: paraelectric tetragonal–paraelectric orthorhombic–ferroelectric orthorhombic for $SrBi_2Ta_2O_9$ and paraelectric tetragonal–ferroelectric orthorhombic–ferroelectric monoclinic for $Bi_4Ti_3O_{12}$. It might be expected that similar arguments would predict analogous symmetry-breaking sequences in other Aurivillius phase with 'even' and 'odd' *n* values. However, precise experimental crystallographic data are still lacking in order to test such models. Only in the case of the $n=2$ ($SrBi_2Ta_2O_9$) and $n=4$ ($SrBi_4Ti_4O_{15}$) phase has the same space group sequence (*I*4/*mmm*–*Amam*–*A*2$_1$*am*) been validated with any certainty [3,12]. For the 'odd' layer materials, even the true nature of the phase

* Corresponding author.
E-mail address: pl@st-and.ac.uk (P. Lightfoot).

0022-4596/$ - see front matter © 2009 Elsevier Inc. All rights reserved.
doi:10.1016/j.jssc.2009.06.038

transition sequence in $Bi_4Ti_3O_{12}$ is still the subject of debate: an intermediate *paraelectric* phase of orthorhombic symmetry has been suggested [9], but has yet to be verified by PND. For the $n = 1$ material Bi_2WO_6, the situation is even more unusual; in this case the parent tetragonal paraelectric phase is not observed; instead a reconstructive transformation occurs at T_C, which destroys the perovskite-like [WO_4] layer arrangement completely [16].

For the $n = 5$ members, structural models have been presented for $A_2Bi_4Ti_5O_{18}$ (A = Ca, Sr, Ba, Pb). Ismunandar et al. [5] proposed an orthorhombic structure, space group B2eb, for the ferroelectric phase of each composition at ambient temperature, whereas Lightfoot et al. [17] suggested that $Ba_2Bi_4Ti_5O_{18}$ remained tetragonal (but polar, space group *I*4*mm*) below T_C. More recently, Tellier et al. [6] supported the B2eb model for $Pb_2Bi_4Ti_5O_{18}$ based on careful electron diffraction studies. $Pb_2Bi_4Ti_5O_{18}$ has been reported to display relaxor ferroelectric behaviour, with a Curie temperature, T_C, or more exactly a frequency-dependent dielectric maximum, T_m, in the vicinity of 285 [18] or 340 °C [19]. In addition, dielectric, heat capacity [20] or piezoelectric [18] anomalies have also been reported around 207–210 °C suggesting a secondary structural phase transition within the ferroelectric regime. Single crystal measurements show that $Pb_2Bi_4Ti_5O_{18}$ retains both *a*-axis and *c*-axis dielectric activity up to T_C [19].

There has been no detailed crystallographic study of any $n = 5$ material at elevated temperature, although Ismunandar et al. [5] plotted lattice parameters versus T for $Pb_2Bi_4Ti_5O_{18}$ and concluded a metrically tetragonal, but crystallographically orthorhombic phase probably occurs above ca. 200 °C, in line with the suggestions of a secondary phase transition from the physical property observations above. The present study is therefore prompted by the above studies, which may suggest that this material undergoes a phase transition sequence distinct from any previously characterised Aurivillius phase.

2. Experimental

$Pb_2Bi_4Ti_5O_{18}$ was prepared by a conventional solid-state reaction of PbO, Bi_2O_3 and TiO_2 for three days at 800 °C followed by one day at 1000 °C in air. Sample purity was confirmed by Rietveld refinement of X-ray powder diffraction data collected on a Stoe STADI/P diffractometer.

Neutron diffraction patterns were collected at 100, 250 and 400 °C on a 5 g sample of $Pb_2Bi_4Ti_5O_{18}$ in a 11 mm vanadium can on HRPD, ISIS Facility, Rutherford Appleton Laboratory, Oxon, UK. These temperatures were chosen to correspond to regions within the three phase fields suggested by earlier studies. The three diffraction patterns were counted for approximately 6 h each. All refinements were performed using the GSAS software suite. Bond valence sums were calculated using Valence [21].

3. Results

Initial Rietveld refinements at 100 °C were performed using the B2eb model previously reported by Ismunandar et al. [5]. An alternative ferroelectric model, using space group *F*2*mm*, was also tested; the fits for both models were very similar and as there were no observable peaks indexed by the B2eb model that were unindexed by the *F*2*mm* model, the higher symmetry *F*2*mm* model is preferred (agreement factors for B2eb: $\chi^2 = 2.34$, $R_{wp} = 2.83\%$ for 96 variables; for *F*2*mm*: $\chi^2 = 2.49$, $R_{wp} = 2.93\%$ for 77 variables. For comparison, the centrosymmetric model, Fmmm gives $\chi^2 = 2.69$, $R_{wp} = 3.04\%$ for 62 variables). Note that alternative models in Fm2m and Fmm2, corresponding to the polarisation along *b* and *c* axes, respectively, were also tested; these models give only marginally poorer fits than *F*2*mm* but are incompatible with previous single crystal measurements of electrical properties, which find the dominant polarisation along the *a* direction. The essential structural difference between these F-centred models and the B2eb model is the absence of octahedral tiltings in the F-centred case. In each model, Bi and Pb were assumed to randomly occupy the perovskite-like A sites, with Bi exclusively occupying the [Bi_2O_2] layer site. It was found that individual isotropic displacement parameters (U_{iso}) were needed for the different oxygen sites, but the Bi/Pb sites and Ti sites had to be constrained to have common values to ensure a stable refinement; this same model for the U_{iso}'s was also used to model the data at 250 and 400 °C. The refined atomic coordinates are given in Supplementary information and the derived bond lengths and bond valence sums (BVS) in Table 1. The refined crystal structure and Rietveld plots are shown in Figs. 1 and 2.

Previous studies [5] found that $Pb_2Bi_4Ti_5O_{18}$ apparently undergoes a structural transition from orthorhombic to metrically tetragonal around 210 °C, which may correspond to the dielectric anomaly reported by Mouri at 207 °C (T_1) [20]. Our diffraction data at 250 °C confirm the lattice is metrically tetragonal above this transition, with *a* and *b* lattice parameters refining as equal within errors, when orthorhombic models were pursued. As we also see no evidence for lowering of symmetry in the lower temperature phase from F-centred to, for example, B-centred, there are no superlattice peaks present to distinguish *metric* tetragonality from *crystallographic* tetragonality. Our data alone, therefore, give no evidence for lowering of symmetry below tetragonal in the 'intermediate' phase, between T_1 and T_m. This implies that the ferroelectric polarisation in this intermediate phase must be along *c*-axis only.

Following the group–subgroup graph for $Bi_4Ti_3O_{12}$ [10], as similar symmetry arguments are applicable for both $n = 3$ and $n = 5$ Aurvilius phases, we conclude that the space group symmetry of the intermediate phase is best described as *I*4*mm*, as the highest symmetry polar tetragonal space group. A good fit was achieved with this model, though only marginally better than the centrosymmetric supergroup *I*4/*mmm* (*I*4*mm*: $\chi^2 = 2.60$,

Table 1
The metal–oxygen bond lengths and bond valence sums (BVS) for $Pb_2Bi_4Ti_5O_{18}$ at 100 °C in space group *F*2*mm*.

Bi1/Pb1–O1 × 2	3.037(9) Å	Bi2/Pb2–O4 × 2	2.7748(15) Å
Bi1/Pb1–O1 × 2	2.795(8) Å	Bi2/Pb2–O4	2.87(3) Å
Bi1/Pb1–O5 × 2	2.7350(5) Å	Bi2/Pb2–O4	2.68(3) Å
Bi1/Pb1–O5	2.79(2) Å	Bi2/Pb2–O6 × 2	3.181(9) Å
Bi1/Pb1–O5	2.69(2) Å	Bi2/Pb2–O6 × 2	3.004(8) Å
Bi1/Pb1–O6 × 2	2.764(9) Å	Bi2/Pb2–O7 × 2	2.494(12) Å
Bi1/Pb1–O6 × 2	2.582(8) Å	Bi2/Pb2–O7 × 2	2.515(12) Å
BVS	2.08	BVS	2.30
Bi3–O2 × 2	2.310(13) Å	Ti1–O1 × 2	2.07(4) Å
Bi3–O2 × 2	2.364(13) Å	Ti1–O1 × 2	1.85(3) Å
Bi3–O3 × 2	2.884(2) Å	Ti1–O5 × 2	2.065(8) Å
Bi3–O3	2.99(2) Å	BVS	3.82
Bi3–O3	2.79(2) Å		
BVS	2.56		
Ti2–O4	1.779(7) Å	Ti3–O3	1.815(7) Å
Ti2–O5	2.125(9) Å	Ti3–O4	2.439(7) Å
Ti2–O6 × 2	2.03(2) Å	Ti3–O7 × 2	1.956(19) Å
Ti2–O6 × 2	1.883(19) Å	Ti3–O7 × 2	1.981(19) Å
BVS	4.32	BVS	3.83
O1 BVS	−1.87	O2 BVS	−2.08
O3 BVS	−1.48	O4 BVS	−1.95
O5 BVS	−1.67	O6 BVS	−1.98
O7 BVS	−2.00		

$R_{wp} = 2.98\%$; $I4/mmm$: $\chi^2 = 2.70$, $R_{wp} = 3.03\%$). We conclude that the 'average structure' of ferroelectric $Pb_2Bi_4Ti_5O_{18}$ can be described in $I4mm$ symmetry in the range $T_1 < T < T_m$. The refined atomic coordinates for this model are given in the Supplementary information and the bond lengths and bond valence sums in Table 2. The final Rietveld plot is shown in Fig. 3.

The third dataset was collected at 400 °C, well within the paraelectric regime. These data were therefore modelled in the archetypal centrosymmetric parent structure, space group $I4/mmm$. The refined atomic coordinates are given in the Supplementary information and the corresponding bond lengths and bond valence sums in Table 3. The final Rietveld plot is shown in Fig. 4.

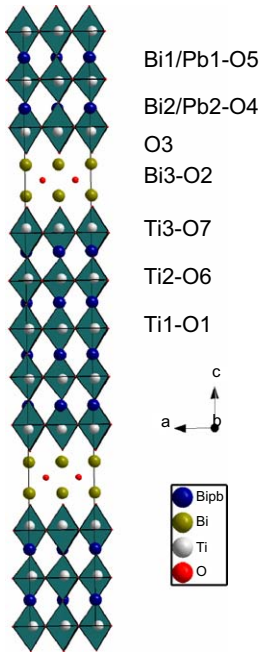

Fig. 1. Crystal structure of $Pb_2Bi_4Ti_5O_{18}$ at 100 °C (space group $F2mm$) viewed along b-axis; note the polar displacements of Ti1 and Ti2 along a.

4. Discussion

Our refinements for both the lower and intermediate temperature phases suggest crystallographic symmetry which is *higher* than that allowed according to the physical property measurements of previous work. Below the transition at T_1, our crystallographic studies have found $Pb_2Bi_4Ti_5O_{18}$ to be orthorhombic. This contrasts with electrical measurements on single crystals [19], where polarisations in both a and c directions require the symmetry to be no higher than monoclinic. In the region $T_1 < T < T_m$ we find the optimum crystallographic fit in the tetragonal, but still polar, space group $I4mm$. This allows polarisation along c but not in the ab plane. A possible rationalisation of these apparently contradictory results may be drawn by considering the effects of 'long-range' versus 'local' structure. $Pb_2Bi_4Ti_5O_{18}$ is known to exhibit relaxor dielectric properties. Relaxor behaviour is believed to arise from localised nano-regions of polarity, which do not fall into register on a longer length scale [22]: for example, the classic relaxor $Pb(Mg_{1/3}Nb_{2/3})O_3$ (PNM) exhibits a cubic, and therefore non-polar crystallographic structure despite showing clear ferroelectric properties [23]. In the present system, Tellier et al. [6] have already reported selected-area electron diffraction (SAED) data which show this type of effect, *viz.* diffuse streaks in certain zones corresponding to those reflections lowering the symmetry from F- to B-centred. They ascribed this to micro-twinning, i.e. twin domains which permute different 90° orientations of locally polar units along a and b axes while keeping c-axis crystallinity intact. This may explain why the present data appear not only as orthorhombic rather than monoclinic, but also as F- rather than B-centred, since the localised regions which exhibit both polarisation and octahedral tilting do not fall into register over the neutron diffraction length scale.

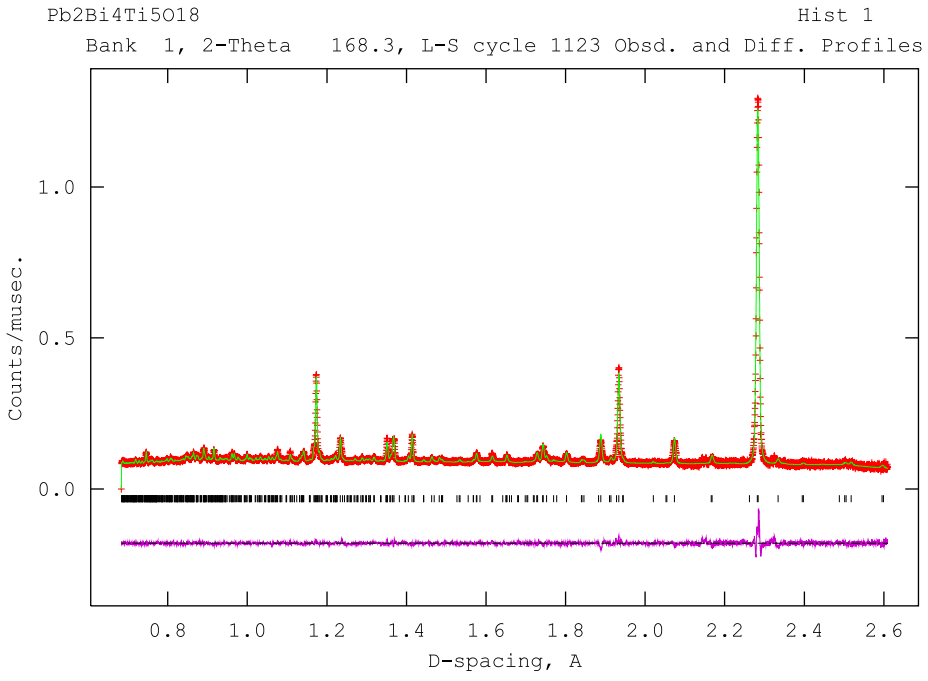

Fig. 2. Final Rietveld fit at 100 °C, space group $F2mm$.

In the previous structural study of $A_2Bi_4Ti_5O_{18}$ (A = Ca, Sr, Ba and Pb) [5], only when A = Ca was there significant tilting of the TiO_6 octahedra, and therefore significant violation of *F2mm* symmetry. The order of tilting of the octahedra was Ca > Sr ≈ Pb > Ba. In this study we find that there was no significant tilting of the TiO_6 octahedra in $Pb_2Bi_4Ti_5O_{18}$ even when refined using B2eb symmetry, and the coordinates refined were closer to the high symmetry special positions of *F2mm* than those obtained in the previous study.

The refined structure of $Pb_2Bi_4Ti_5O_{18}$ at 100 °C is shown in Fig. 1 and Table 1 (see also Supplementary for CIF data). The major polar distortions (compared to idealised non-polar Fmmm parent structure) are the negative Δx values for Ti1 and Ti2, plus the positive Δx for O1 (which is in the same plane perpendicular to c as Ti1, i.e. the central octahedral layer). The polar distortions of the TiO_6 octahedra involve the displacement of the Ti^{4+} cation towards an edge of the octahedron. According to our results this occurs predominantly in the middle three of the five layers of the perovskite block, with the central layer (including Ti1 and O1) having the largest ferroelectric polarisations. The distortions in the fluorite layer and those of the perovskite A cations are small in

Table 2
The metal–oxygen bond lengths and bond valence sums (BVS) for $Pb_2Bi_4Ti_5O_{18}$ at 250 °C in space group *I4mm*.

Bi1/Pb1–O1 × 4	2.95(2) Å	Bi1a/Pb1a–O1 × 4	2.85(2) Å
Bi1/Pb1–O5a × 4	2.7503(14) Å	Bi1a/Pb1a–O5 × 4	2.7381(5) Å
Bi1/Pb1–O6 × 4	2.634(12) Å	Bi1a/Pb1a–O6a × 4	2.770(12) Å
BVS	2.06	BVS	1.91
Bi2/Pb2–O4a × 4	2.7485(19) Å	Bi2a/Pb2a–O4 × 4	2.833(5) Å
Bi2/Pb2–O6 × 4	3.016(13) Å	Bi2a/Pb2a–O6a × 4	3.248(14) Å
Bi2/Pb2–O7a × 4	2.645(11) Å	Bi2a/Pb2a–O7 × 4	2.362(7) Å
BVS	1.96	BVS	2.72
Bi3–O2 × 4	2.488(9) Å	Bi3a–O2 × 4	2.233(7) Å
Bi3–O3a × 4	2.857(5) Å	Bi3a–O3 × 4	2.941(7) Å
BVS	1.89	BVS	3.15
Ti1–O1 × 4	1.9394(17) Å		
Ti1–O5	2.15(2) Å		
Ti1–O5a	1.834(19) Å		
BVS	4.21		
Ti2–O4	1.827(19) Å	Ti2a–O4a	1.79(2) Å
Ti2–O5	2.10(3) Å	Ti2a–O5a	2.327(18) Å
Ti2–O6a × 4	1.9362(5) Å	Ti2a–O6 × 4	1.955(3) Å
BVS	4.32	BVS	4.05
Ti3–O3	1.82(2) Å	Ti3a–O3a	1.75(2) Å
Ti3–O4	2.42(2) Å	Ti3a–O4a	2.36(3) Å
Ti3–O7 × 4	1.964(3) Å	Ti3a–O7a × 4	1.956(3) Å
BVS	3.85	BVS	4.13
O1 BVS	−1.90		
O2 BVS	−2.06		
O3 BVS	−1.39	O3a BVS	−1.45
O4 BVS	−1.72	O4a BVS	−1.99
O5 BVS	−1.59	O5a BVS	−1.90
O6 BVS	−2.02	O6a BVS	−1.86
O7 BVS	−2.33	O7a BVS	−1.82

Table 3
The metal–oxygen bond lengths and bond valence sums (BVS) for $Pb_2Bi_4Ti_5O_{18}$ at 400 °C in space group *I4/mmm*.

Bi1/Pb1–O1 × 4	2.931(4) Å	Bi2/Pb2–O4 × 4	2.7843(12) Å
Bi1/Pb1–O5 × 4	2.7471(5) Å	Bi2/Pb2–O6 × 4	3.121(4) Å
Bi1/Pb1–O6 × 4	2.671(4) Å	Bi2/Pb2–O7 × 4	2.486(3) Å
BVS	1.99	BVS	2.31
Bi3–O2 × 4	2.350(2) Å	Ti1–O1 × 4	1.93876(2) Å
Bi3–O3 × 4	2.893(2)	Ti1–O5 × 2	2.028(7) Å
BVS	2.47	BVS	3.68
Ti2–O4	1.770(9) Å	Ti3–O3	1.824(8) Å
Ti2–O5	2.199(10) Å	Ti3–O4	2.429(9) Å
Ti2–O6 × 4	1.9483(8) Å	Ti3–O7 × 4	1.9772(15) Å
BVS	4.27	BVS	3.75
O1 BVS	−1.86	O2 BVS	−2.00
O3 BVS	−1.53	O4 BVS	−1.95
O5 BVS	−1.62	O6 BVS	−1.95
O7 BVS	−2.00		

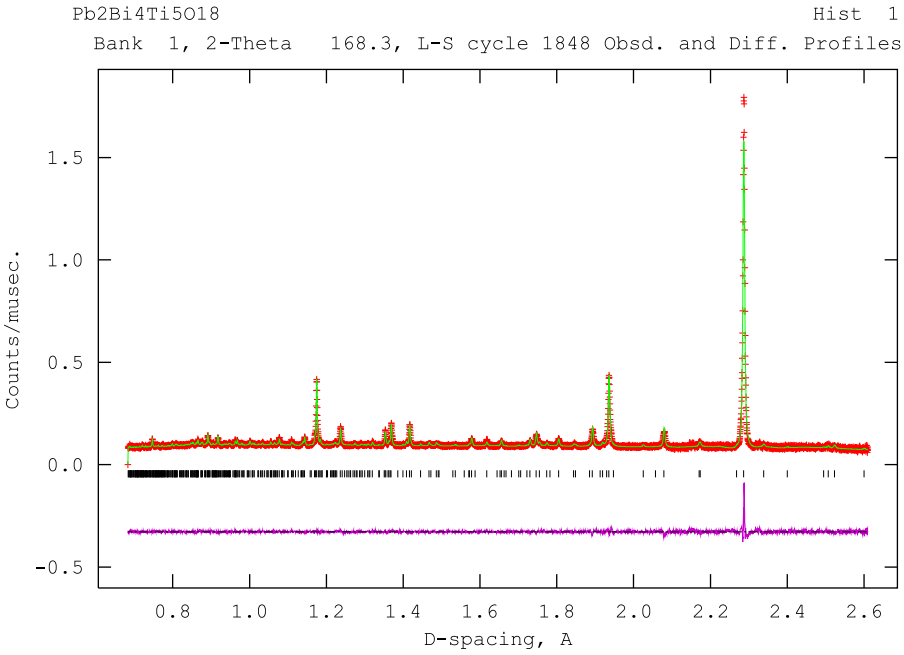

Fig. 3. Final Rietveld fit at 250 °C, space group *I4mm*.

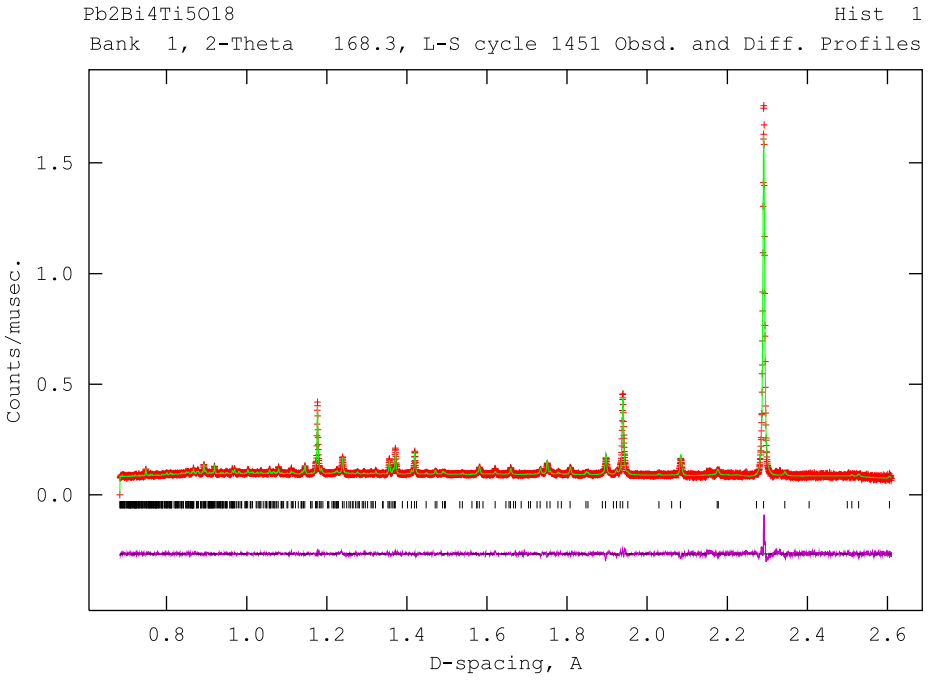

Fig. 4. Final Rietveld fit at 400 °C, space group *I*4/*mmm*.

comparison to those of the TiO_6 octahedra. From the data we have it is not reasonable to speculate on the nature of the monoclinic distortion suggested from the physical property measurements. However, an extremely subtle monoclinic distortion also occurs in the $n=3$ phase $Bi_4Ti_3O_{12}$ [7]. It was suggested to arise from an additional tilting mode of the central octahedral block around *c*-axis, which removes a 2-fold axis and reduces the symmetry from orthorhombic B2eb to monoclinic B1a1. This has been supported by the theoretical study of Perez-Mato et al. [10].

Based on our current model in *F*2*mm* symmetry, the total *a*-axis polarisation, calculated using the point charge method [4] is 8.4 μC/cm^2, which is in modest agreement with the value of 17 μC/cm^2 found experimentally [19]. The corresponding *c*-axis polarisation observed experimentally is only 0.7 μC/cm^2, which emphasises the subtle nature of the apparent monoclinic distortion.

In the intermediate phase in the region $T_1<T<T_m$ (refined at 250 °C, tetragonal *I*4*mm*) the only net long-range polarisation must switch from the *a* to the *c* direction. This is, of course, at odds with single crystal electrical measurements which find that the dielectric constant along *a* remains much higher than that along *c* above this transition. Nevertheless, we see no direct evidence for lowering of the long-range crystallographic symmetry, but we do see a modest improvement in fit between *I*4*mm* and *I*4/*mmm* (centrosymmetric) models. In this model, the main polar distortions (relative to *I*4/*mmm*) originate from *c*-axis shifts of the Bi^{3+} cations in the fluorite layer and in the outer layer of A site cations in the perovskite blocks. The total polarisation in this model is calculated as 3.5 μC/cm^2. The pattern of distortions of the two outer layers of TiO_6 octahedra remains the same as at lower temperatures, but now there is no net cancellation due to the change in symmetry.

In the refined *I*4/*mmm* structure above T_m at 400 °C, the pattern of equal and opposite Ti^{4+} displacements along *c* in the outer two layers of the perovskite blocks remains, and the middle layer is now in a more symmetric environment. The A site cations are also shifted towards the outside of the perovskite blocks with equal and opposite magnitudes.

The calculated bond valence sums (shown in Tables 1–3) support the assumption that the fluorite layers are fully occupied by Bi, and that the perovskite A sites contain random Bi/Pb occupancy, as the fluorite layer BVS is significantly higher than those of the A sites in both *F*2*mm* and *I*4/*mmm*.

In summary, a powder neutron diffraction investigation suggests the phase transition sequence *F*2*mm*→*I*4*mm*→*I*4/*mmm* as a function of increasing temperature, for the three phases of $Pb_2Bi_4Ti_5O_{18}$. This is a unique transition sequence for an Aurivillius phase, and is at odds with both electrical measurements and SAED (a more local structural probe). This points towards structural behaviour characteristic of a relaxor ferroelectric, whereby the long-range crystallographic symmetry is not representative of the true, short-range polar order. If the true symmetry of $Pb_2Bi_4Ti_5O_{18}$ below T_m is indeed monoclinic, then it may manifest only in the 'average' structure by extremely subtle effects, even more subtle than those seen in the $n=3$ analogue $Bi_4Ti_3O_{12}$. In that case, the lowering of symmetry may be best seen in the anisotropic atomic displacement parameters of certain O atoms, specifically those in the plane of the central Ti layer, which relate to an additional octahedral tilt mode. In the present case the O1 atom in the central octahedral layer again has consistently the largest displacement parameter; however, it is not reasonable to model this behaviour in terms of lower symmetry. Clarification of such a phenomenon is beyond the scope of the present data, and may require single crystal neutron diffraction of the highest quality.

Acknowledgments

We thank Dr Kevin Knight and Ms Alex Gibbs for assistance in neutron data collection at ISIS, and EPSRC for funding.

Appendix 1. Supporting Information

Supplementary data associated with this article can be found in the online version at doi:10.1016/j.jssc.2009.06.038.

References

[1] B. Aurivillius, Arkiv. Kemi. 1 (1949) 463.
[2] C.A.P. de Araujo, J.D. Cuchlaro, L.D. McMillan, M. Scott, J.F. Scott, Nature (London) 374 (1995) 627.
[3] C.H. Hervoches, J.T.S. Irvine, P. Lightfoot, Phys. Rev. B. 64 (2001) 100102(R).
[4] Y. Shimakawa, Y. Kubo, Y. Nakagawa, S. Goto, T. Kamiyama, H. Asano, F. Izumi, Phys. Rev. B. 61 (2000) 6559.
[5] P. Ismunandar, T. Kamiyama, A. Hoshikawa, Q. Zhou, B.J. Kennedy, Y. Kubota, K. Kato, J. Solid State Chem. 177 (2004) 4188.
[6] J. Tellier, P. Boullay, D. Mercurio, Z. Kristallogr. 222 (2007) 234.
[7] A.D. Rae, J.G. Thompson, R.L. Withers, A.C. Willis, Acta Crystallogr. B 46 (1990) 474.
[8] P. Boullay, G. Trolliard, D. Mercurio, L. Elcoro, J.M. Perez-Mato, J. Solid State Chem. 164 (2002) 261.
[9] Q.D. Zhou, B.J. Kennedy, C.J. Howard, Chem. Mater. 15 (2003) 5025.
[10] J.M. Perez-Mato, P. Blaha, K. Schwarz, M. Aroyo, D. Orobengoa, I. Extebarria, A. Garcia, Phys. Rev. B. 77 (2008) 184104.
[11] I.M. Reaney, M. Roulin, H.S. Shulman, N. Setter, Ferroelectrics 167 (1995) 295.
[12] C.H. Hervoches, A. Snedden, R. Riggs, S.H. Kilcoyne, P. Manuel, P. Lightfoot, J. Solid State Chem. 164 (2002) 280.
[13] A. Snedden, C.H. Hervoches, P. Lightfoot, Phys. Rev. B. 67 (2003) 092102.
[14] N.C. Hyatt, I.M. Reaney, K.S. Knight, Phys. Rev. B. 71 (2005) 024119.
[15] J.M. Perez-Mato, M. Aroyo, A. Garcia, P. Blaha, K. Schwarz, J. Schweifer, K. Parlinksi, Phys. Rev. B. 70 (2004) 214111.
[16] N.A. McDowell, K.S. Knight, P. Lightfoot, Chem. Eur. J. 12 (2006) 1493.
[17] P. Lightfoot, A. Snedden, S.M. Blake, K.S. Knight, Mater. Res. Soc. Symp. Proc. 755 (2003) 89.
[18] J.F. Fernandez, A.C. Caballero, M. Villegas, J. De Frutos, L. Lascano, Appl. Phys. Lett. 81 (2002) 4811.
[19] I.-N. Yi, M. Miyayama, J. Ceram. Soc. Jpn. 106 (1998) 285.
[20] S. Mouri, M. Fukunaga, S. Hiramatsu, M. Takesada, H. Satoh, A. Onodera, Ferroelectrics 35 (2007) 50.
[21] I.D. Brown, J. Appl. Crystallogr. 29 (1996) 479.
[22] Z.G. Ye, Key Eng. Mater. 155–1 (1998) 81.
[23] P. Bonneau, P. Garnier, G. Calvarin, E. Husson, J.R. Gavarri, A.W. Hewat, A. Morrell, J. Solid State Chem. 92 (1991) 350.